Experimental observation and realistic modelingof initiation and propagation of the rock fracture by acoustic emission

Shuhong Wang[1,2], Chung-in Lee[1], Seok-won Jeon[1], Heekwang Lee[1], Chun-an Tang[3]

[1] School of Civil, Urban & Geosystem Engineering, Seoul National University, Seoul, 151744, Korea
[2] School of Resource and Civil Engineering, Northeastern University, Shenyang, 110004, China;
[3] Research Institute of Engineering Mechanics, Dalian University of Technology, Dalian, 116024, China

Abstract

It is well known that acoustic emission (AE) is indicator of rock fracturing or damage as rock is brought to failure under the uniaxial compressive loads. In this paper, an experimental study on the source location of acoustic emission on the cylindrical specimens of granite under uniaxial compression test was made. The AE source location was made by measuring the six channel AE data. Comparing to this experiment, the numerical method is applied to model the initiation and propagation of fracture by AE using a numerical code, RFPA (Realistic Failure Process Analysis). This code incorporates the mesoscopic heterogeneity in Young's modulus and rock strength characteristic of rock masses. In the numerical models, values of Young's modulus and rock strength are realized according to a Weibull distribution in which the distribution parameters represent the level of heterogeneity of the medium. The results of the simulations show that RFPA can be used not only to produce acoustic emission similar to those measurements in our experiments, but also to predict fracturing patterns under uniaxial loading condition.

Key words

Acoustic emission Damage; Microcracking; Rock Numerical modelling; Fracture process; Heterogeneity; initiation and propagation of the rock fracture

1. Introduction

With the development of many rock engineerings, such as tunnels and underground caverns, the fracture or failure of rock has been the subject of extensive researches in an excavation disturbed or damaged zone (EDZ) around rock underground, the results of which have led to a number of comprehensive texts [1-4]. The formation of the EDZ is affected by various factors, such as stress redistribution and excavation methods. Nowdays, acoustic emission (AE) techniques are broadly applied to rock to obtain the information on crack initiation and propagation in these rock engineerings [5-7], However, despite the extensive work and the numerous successes in predicting fracture behaviour, our understanding of the physical processes that ultimately control fracture behaviour is weak (Landis, 1999). Although to some extent we are able to predict failure loads and damage patterns, we still do not have a good understanding of the material fabric characteristics and their influence on the subsequent progressive fracture process. For rock materials, heterogeneity is an example of such kinds of material fabric characteristics. It logically follows that if we have a better understanding of heterogeneity, we will be in a better position to formulate predictive models and predict the rock fracture behaviour. At present, it is impossible or difficult for theoretical or analytical methods to research the fracture behaviours of rock incorporating heterogeneity and anisotropy. From this point of view, the numerical tool is a good means of gaining some insights into the problem of the heterogeneous and anisotropic rock fracture propagation.

The numerical simulation of the fracture process requires robust numerical methods that can allow the efficient resolution of multiple interacting cracks and rigorous material models that can reflect the material fabric characteristics, i.e. the heterogeneity for rock materials. In fact, during the past few years with the rapid development of computing power, interactive computer graphics and topological data structure, a large number of numerical methods incorporating heterogeneous material models have been developed for research on the rock fracture process, such as the studies of Tang (1997), Blair and Cook (1998), Tang and Kaiser (1998) and Liu et al (2002). From the numerical methods and material models introduced above, it seems that the numerical method developed on the basis of the finite element method and the statistical material model is appropriate for research on the rock fracture problem.

In previous papers [8], a heterogeneous material model has been proposed to characterize rock heterogeneity according to the Weibull statistical theory and fully implemented into the rock and tool RFPA, which is developed on the basis of the finite element method (FEM).

In this paper, the measurements of acoustic emission and the source location were conducted on granite specimens under uniaxial compression. And another experimental result [1] is also presented for comparing with our experimental and numerical results. The numerical analysis was conducted using numerical tool RFPA code coupled with a heterogeneous and anistropic material. It is conclused that the simulated results using RFPA code were similar tendency to the experimental results and could obtain the crack initiation, propagation, and whole progressive fracture process.

2 Experimental set-up and procedures

2.1. Samplespreparation

Granite produced at Gyunggi province in Korea was the rock types that were used for testing.The Granite specimens for physical properties test are the core samples with 52-53mm in diameter. The sample preparation and testingprocedure are according to the standard testing of ISRM. Their physical and mechanical properties are summarized in Table 1.

The samples were prepared in the rock engineering laboratory in Seoul National University. The ratio of height to diameter of the specimens was 2.15 (see in Fig.1). Both ends of specimens were ground parallel to within 0.02mm and specimens were dried at 105°C before testing.

Table 1. Physical and mechanical properties of rock samples

Properties	Units	Granite
Specific gravity		2.67
Apparent porosity	%	0.79
P-wave velocity	m/s	3770
S-wave velocity	m/s	2250
Uniaxial compressive strength	MPa	99.3
Young's modulus	GPa	42.4
Posson's ratio		0.25

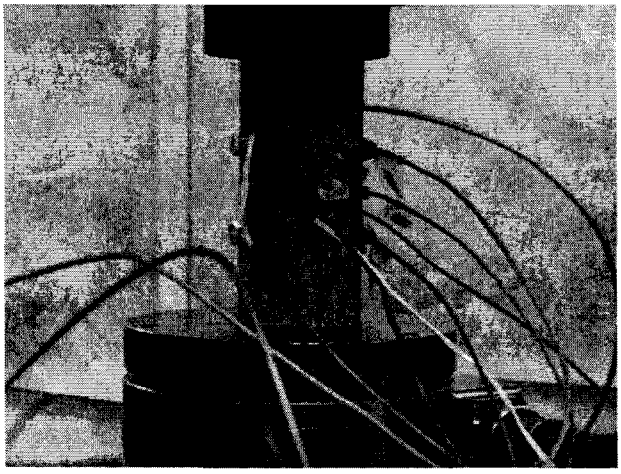

Fig. 1 The sample with 6 sensors

2.2. Testing equipments

The test was performed using a universal testing machine, Shimadzu UDH-200A. And the data acquisition system, system 5000, was used torecord load and displacement every 0.2 seconds. At the same time, an Acoustic Emission System, Mistras 2001, was adopted to detect damage and fracture of rock samples, and a Digital Camera was used to record the cases of crack initiation, crack propagation and failure patterns of the specimens. Fig. 2 shows each testing equipment used during the uniaxial compressive test

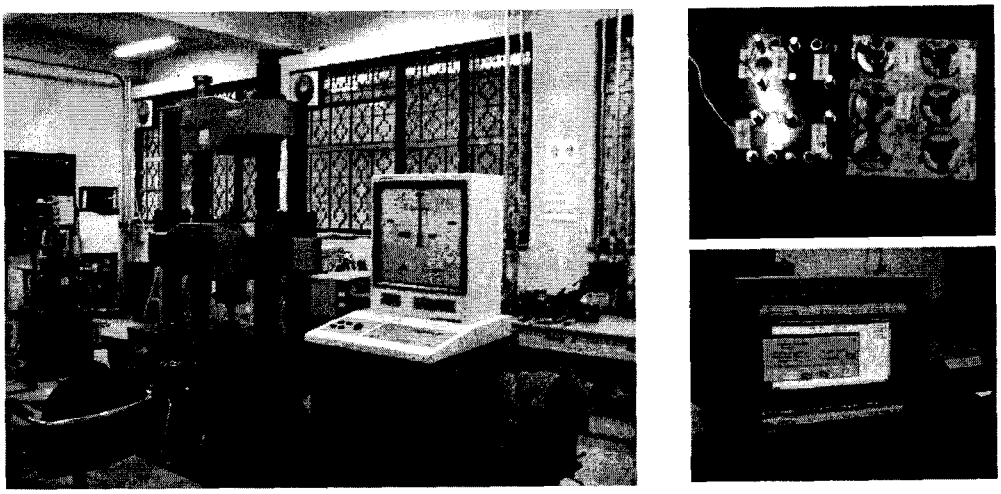

Fig. 2 The part testing equipments

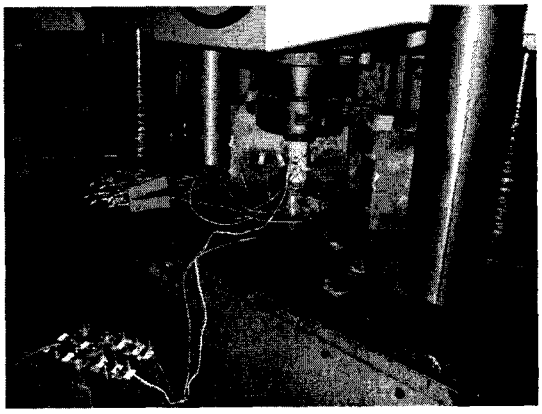

Fig.3 The sample

The diameter and the thickness of AE sensors (HagiSonic, Korea) were 3.6 and 2.4 mm, respectively. The main frequency band of the AE sensors was between 100 kHz and 1 MHz. To easily attach AE sensors to samples and obtain the same sensitivity for each sensor, an electron wax was used. AE signals measured in the sensors were amplified by 40 dB with pre-amplifiers (PAC model 1220A). Fig. 3 shows the sample before loading to which attached by sensors and strain gauge. The mechanical and acoustic emission (AE) measurements were conducted in the conventional uniaxial compressive test configuration.

Fig. 4 shows the location of 6 sensors attached to the specimen during the uniaxial compressive testto perform the AE source location. Sensors are attached in each 4 vertical line of the sample in which 2 sensors are at the 1/3 and 2/3 points of the opposite 2 vertical lines and 1 sensor at the 1/2 point in another 2 lines shown in Fig. 4.

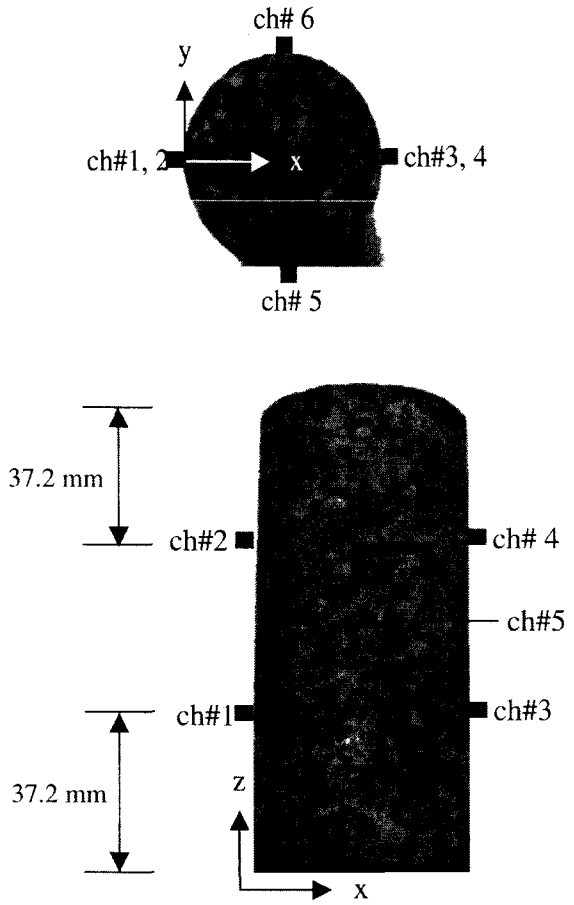

Fig.4 The Arrangement of AE sensors for AE analysis and AE source location under uniaxial compression

2.3 Experimental procedures

During the uniaxial compression test, the rate of displacement was controlled to 1 mm/min. In addition, the MISTRAS 2001 system manufactured by the Physical Acoustic Corporation (PAC) was used for the AE measurements. Considering background noise, the AE trigger level was set to 40 dB. Time parameters for AE wave forms include Peak Definition Time (PDT), Hit Definition Time (HDT) and Hit Locking Time (HLT).

2.4 Experimental results

2.4.1 AE characteristics in uniaxial compression

The correlations between AE events and the stress-strain curves of rock samples are shown in Fig. 5. It was found that the occurrence of AE had a good correlation with the load versus the deflection curve.

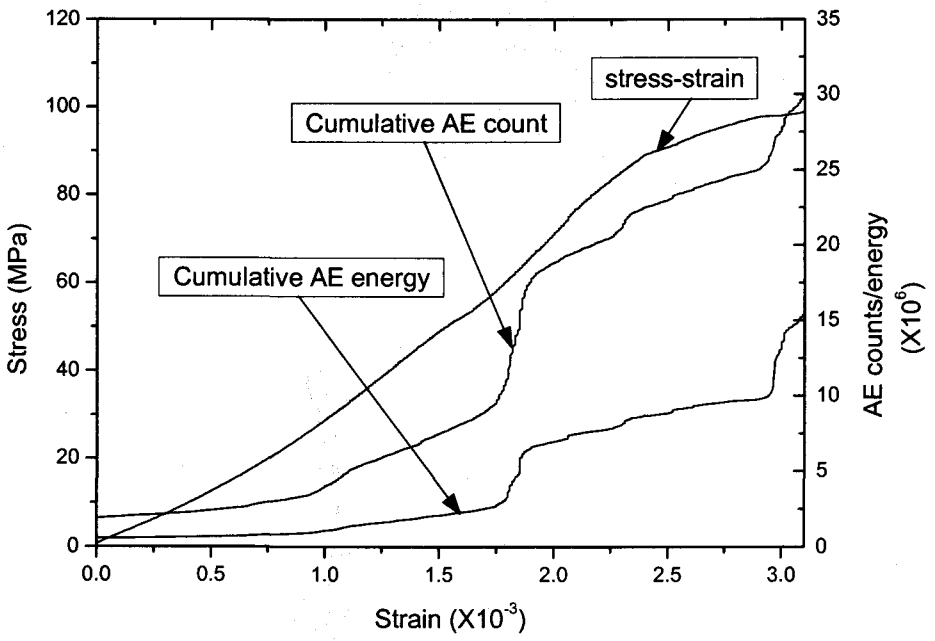

Fig.5 The stress-strain curve and AE counts (energy release) in rock sample.

In the ascending branch of the load-displacement curves, the AE characteristics of rock samples were similar:

(1) During the initial loading stage, there was little occurrence of AE activities;

(2) As the load reached about 60% of the failure load, the AE activity became more intense;

(3) When the external load approaches the ultimate strength, the AE activity increased rapidly.

The position of the peak shifted to the latter part of the descending branch of the load-displacement curves. What need to say, according to the statistical theory of damage of quasibrittle materials, rockcan be considered to be composed of many microelements. Under the external load, the rupture probability of each microelement is different but normally complies with a Weibull distribution.

Fig. 6 shows the AE source location, which is 2 dimensional view, when the external load is

about the ultimate strength. The locations are mainly distributed in the diagonal direction in xz plane of Fig. 6 (b) bounding from upper right to lower left and there many in the middle of the sample, where the failure occurs shown in Fig. 6 (a). The size of the circle is the amplitude of the AE source and larger source is mainly distributed in the middle part of the sample in both xz and yz plane. It is shown that the failure planes shown in Fig. 10 are coincidence with the AE source locations (Fig. 6(b)).

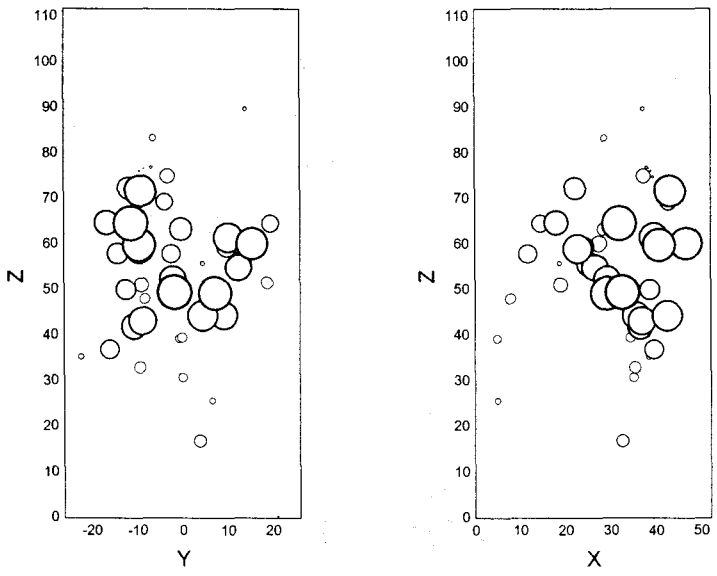

(a) YZ plane (b) XZ plane

Fig. 6 Plot of AE source location (2D)

Fig. 7 shows another case of AE source locations for the Hwang-Deung granite conducted by Chang S.-H. and Lee C. I[1]. The AE sources were scattered at a low stress level (Fig. 7(a)). However, as the stress increased, they were concentrated around the failure planes (Fig. 7 (b) and (c)). Especially, above the crack damage stress level, AE sources were concentrated around the center of a rock specimen.

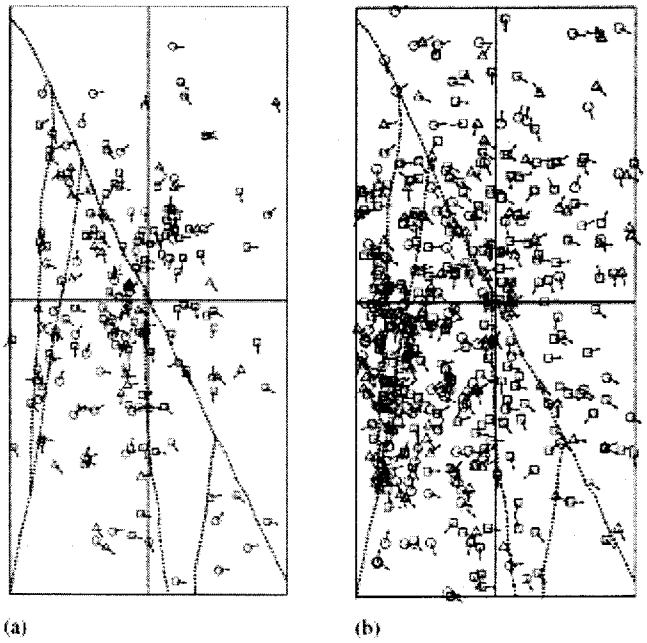

Fig. 7 AE source locations in a granite sample under uniaxial compression ((□): shear crack, (○): tensile crack, (△): mixed-mode crack, (→): crack motion vector): (a) $\sigma_{ci} \sim \sigma_{cs}$ (b) $\sigma_{cs} \sim \sigma_{cd}$ and (c) $\sigma_{cd} \sim$ post-peak (After Chang S.-H.,and Lee C. -I.[1])

The overall failure mechanism of rock could be well estimated by the relative crack volumes representing the damage index. Fig. 8 shows that AE sources with large relative crack volumes during the uniaxial compression test were located near failure plane (Chang S. -H., and Lee C. -I. [1]).

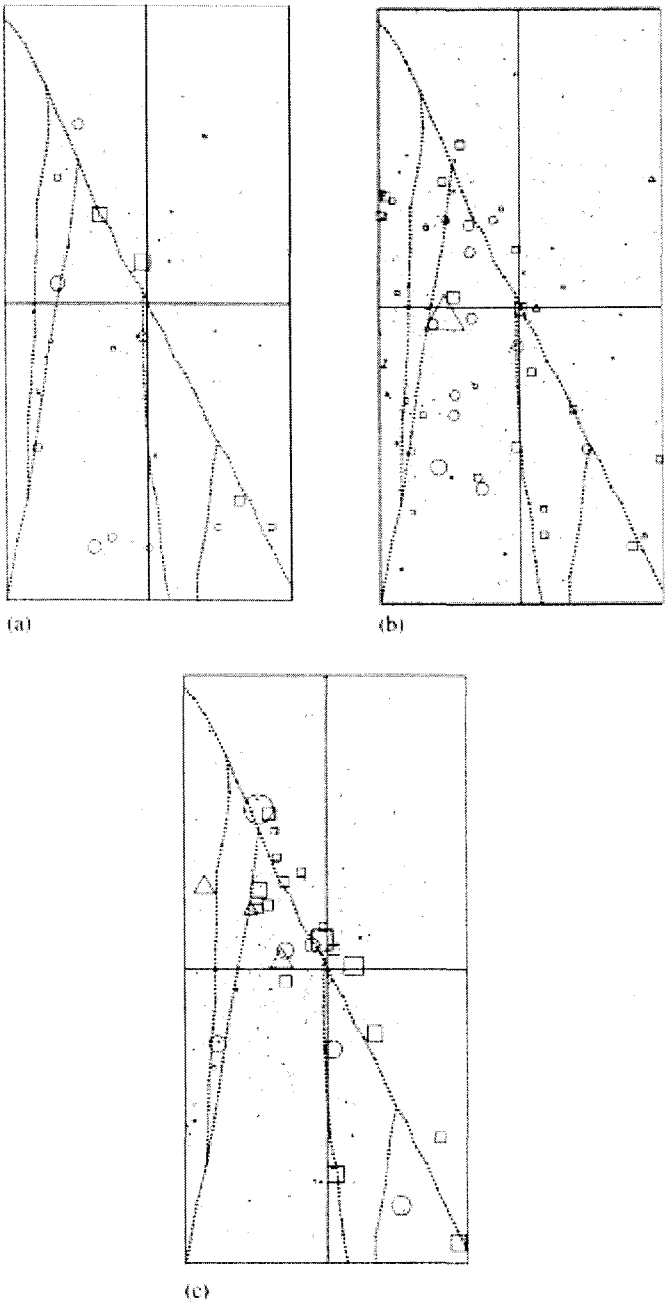

Fig. 8 AE source locations with different symbol sizes representing relative crack volume in a granite sample under uniaxial compression test ((□): shear crack, (○): tensile crack, (△): mixed-mode crack, (→): crack motion vector): (a) $\sigma_{ci} \sim \sigma_{cs}$; (b) $\sigma_{cs} \sim \sigma_{cd}$; and (c) $\sigma_{cd} \sim$ post-peak (After Chang S.-H.,and Lee C. -I.[1]).

3. Brief description of numerical method

As introduced in previous papers (Tang, 1997, Liu et al, 2002; Wang, 2004), a heterogeneous

material model has been proposed to characterize heterogeneous rock material as the homogeneous index m and the elemental seed parameters, i.e. the mean values of the main physical-mechanical parameter: critical strength, σ_0, elastic modulus, E_0, etc according to the Weibull statistical distribution:

$$\varphi(\varepsilon)=\frac{m}{\varepsilon_0}\left(\frac{\varepsilon}{\varepsilon_0}\right)^m \exp\left[-\left(\frac{\varepsilon}{\varepsilon_0}\right)^m\right] \tag{1}$$

where ε is the elemental parameter, ε_0 is the elemental seed parameter and m is the homogeneous index . The elemental seed parameters corresponding to any specific rock can be obtained from the main physical-mechanical parameters in a laboratory test, and the homogeneous index m can be determined on the basis of the defect distribution of the microstructure (Orlovskaja et al, 1997; Curtis and Juszczyk, 1998; Davies, 2001).

The heterogeneous material model has been fully implemented into the RFPA code developed on the basis of the FEM and the RFPA model (Tang, 1997). The main contents of the RFPA code include the heterogeneous material model, the Mohr-Coulomb criterion and the elastic damage mesoscopic elemental mechanical constitutive law.

In the numerical simulation, the numerical model is constructed on the basis of the heterogeneous material model. An external load is slowly applied on the constructed numerical model step by step. The finite element method is used to compute the stress and deformation in each element ofthe built numerical model. The Mohr-Coulomb criterion is used to examine whether or not the elements undergo a phase transition. When in a certain step the stresses in some elements satisfy the strength criterion, the elements are damaged and become weak according to the rule specified by the elastic damage mesoscopic elemental mechanical constitutive law. The stress and deformation distributions throughout the model are then adjusted instantaneously after each rupture to reach the equilibrium state. At positions with an increased stress due to stress redistribution, the stress may satisfy the critical value and further ruptures are caused. The process is repeated until no failure elements are present. The external load is then increased further. In this way the system develops a macroscopic fracture. Thus the code links the mesoscopic mechanical model to the continuum damage model and ultimately to the macrostructure failure. Energy is stored in the element during the loading process and is released as acoustic emission (AE) through the onset of elemental failure. Due to the interaction induced by stress redistribution and long-range deformation, a single important element failure may cause an avalanche of additional failures in neighbouring elements, leading to a chain reaction releasing more energy.

4. Numerical modelling of the fracture processes in basic rock mechanics experiments

In the laboratory, basic rock mechanics experiments are conducted to obtain the physical-

mechanical properties. The physical-mechanical properties of rock material mainly include the uniaxial compressive strength, tensile strength and elastic modulus, etc. The uniaxial compressive strength test are usually adopted to obtain these physical - mechanical parameters. The testing techniques usually follow the recommendations given in the methods suggested by ISRM (ISRM, 1978 and 1979).

The rapid expansion of research in fracture mechanics has also concerned rock fracture. The most fundamental parameter in fracture mechanics is fracturetoughness, which describes the resistance of a material to crack propagation. Fracture toughness is defined as the critical value of the stress intensity factor (SIF) when crack initiation takes place.

In this paper, Numerical specimens for the uniaxial compressive strength (UCS) test isconstructed with the same characteristic parameters of the heterogeneous material model to simulate the progressive fracture process and determine the local physical-mechanical properties and fracture toughness.

While building numericalmodel, the following main characteristic parameters are used: the homogeneous index is $m = 2$ which is a typical value for the heterogeneous rocks according to the heterogeneous material model and the elemental seed parameters, i.e. the mean value of the compressive strength is 0 = 200 *MPa*, the mean value of the elastic modulus is $E_0 = 60$ *GPa*. We further assume here that the Poisson's ratio is 0.25 and a fixed ratio (0.1) exists between the tensile strength and the uniaxial compressive strength of the rocks. On the basis of these parameters, we can use granite, a typical heterogeneous material.

In some of the aforementioned numerical experiments, loading plates or loading points are needed. In order to prevent the permanent deformation of the loading plates or loading points and get rid of their influence, their strength and elastic modulus are 5-6times higher than those of the built specimen. Corresponding values are also given to the other parameters. The homogeneous index for the loading plates or loading points is very high (1000). Accordingto the heterogeneous model, when the homogeneous index is high, the constructed object is homogeneous. Therefore, the loading plate or loading point is modelled as a homogeneous material with a high strength compared with the rock, whereas the rock is modelled as a heterogeneous material.

From all of these numerical experiments, if we can observe reasonable progressive fracture processes and obtain relatively accurate values for the physical-mechanical properties and fracture toughness compared with experimental results, we can confidently conclude that the heterogeneous rock can be characterized according to the heterogeneous material model and the RFPA code is a valuable numerical tool to perform research on the rock progressive fracture process.

Note that throughout this paper, following the regulations in rock mechanics, compressive stresses and strains are taken as positive, while on the other hand, tensile stresses and expansionary strains are taken as negative.

The UCS test is simplified as a plane stress problem and a vertical section is considered. The numerical model is built according to the geometry suggested by ISRM, i.e. the diameter D = 52 mm and the ratio between the height and the diameter H/D = 2.15. As mentioned earlier, the

numerical model is constructed on the basis of the heterogeneous material model: the homogeneous index (m = 2), the elemental seed parameters the mean values of compressive strength ($\sigma_0 = 200MPa$) and elastic modulus ($E_0 = 60GPa$) and so on (see in Fig.7). The load at a constant displacement increment of 0.002 mm/step is applied in the vertical direction. The specimen is loaded up to failure, and the whole force-displacement curve is recorded.

The numerical simulation of the UCS test is relatively simple. Since a previous paper (Tang et al, 2000) has discussed it in detail, herein just the results are reported briefly. Fig. 10 shows the simulated force-loading displacement curve and associated AE. The curve has a substantial linear region (line before Point A), a non-inearity (OA) region and a clear post-peak region (BCD: strain softening).

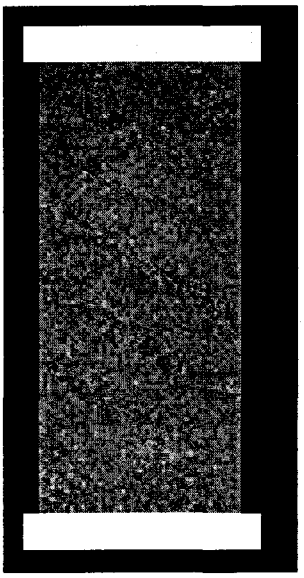

Fig. 9 The numerical model

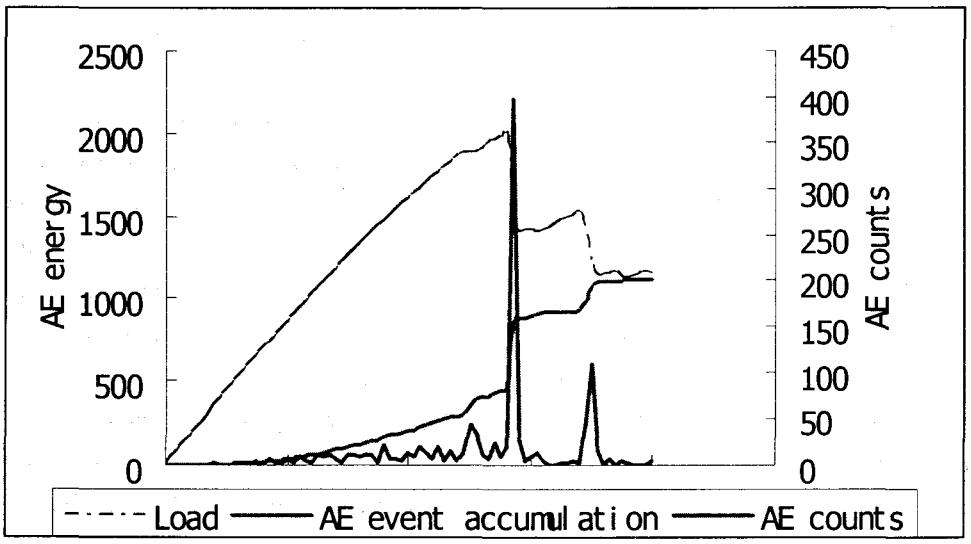

Fig. 10 Force-loading displacement curve and associated AE events induced by the UCS test

The associated event rates are shown as a histogram in Fig. 10. The event rates show that during the initial deformation or linear-elastic phase (before Point A), little elastic energy is released, although some failure eventsoccur because of heterogeneity. An increasing rate of failure events accompanies the inelastic phase (AB) and failure stage (BCDE). According to the peak load P_{max} of the force-loading displacement curve (Point B), we can calculate the uniaxial compressive strength as Eq. 2:

$$\sigma = \frac{P_{max}}{A} = \frac{1993.854}{(52 \times 0.2) \times 1} = 191.8MPa \tag{2}$$

In the linear part of the force-loading displacement curve (before Point A), the axial force change $\Delta P = 1181.557N$ and the axial specimen shortening displacement $\Delta l = 0.04mm$. Therefore, the elastic modulus can be calculated as Eq. 3:

$$E = \frac{\Delta\sigma}{\Delta\varepsilon} = \frac{1181.557}{(52 \times 0.2) \times 1} \Big/ \frac{0.04}{20} = 568075.55MPa = 56.8GPa \tag{3}$$

In comparison with the experimental data (σ = 99.3 *MPa* and E = 42.4 *GPa*) for the reference rock, the simulated uniaxial compressive strength and elastic modulusare relatively accurate. Because rock heterogeneity is considered in the model, there are small variances between the simulated data and the experimental data for the reference granite.

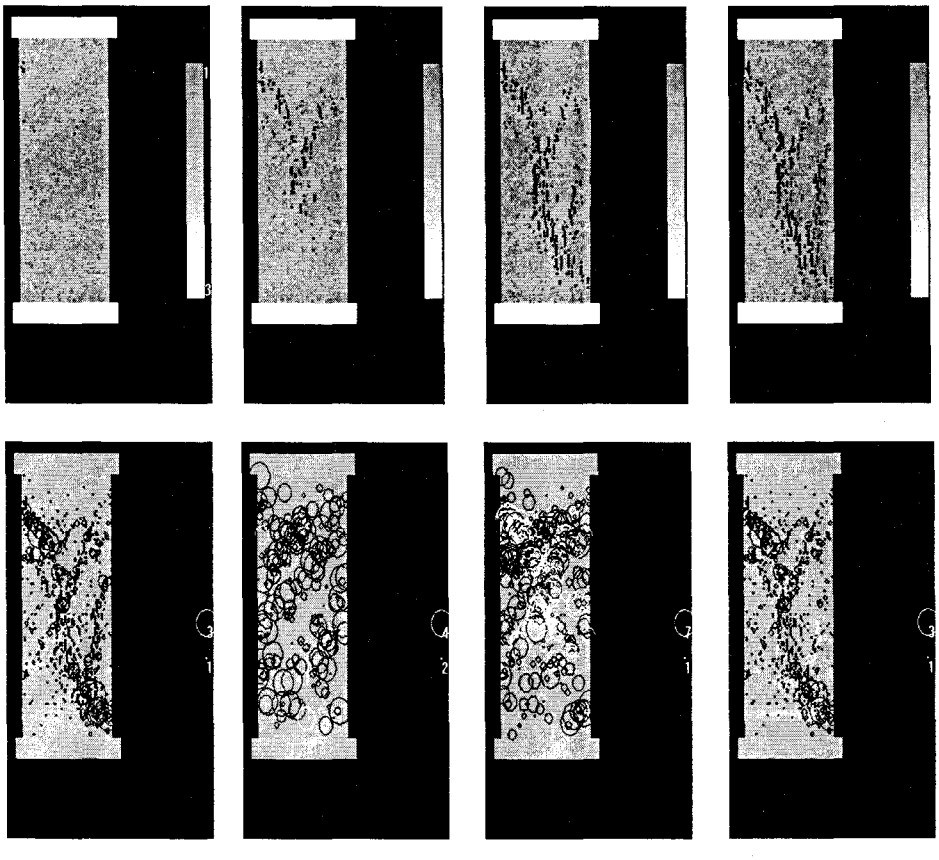

Fig. 11 Progressive fracture process induced by the UCS test

Fig. 11 shows the simulated initiation, propagation and coalescence of the fractures at different loading levels. The letters in the figure correspond to those in Fig. 8, which indicate the different loading levels. It can be seen that the onset of failure in the specimen subjected to uniaxial compressive loading is firstly indicated by the formation of a large number of isolated microfractures and then the microfractures begin to cluster and become clearly localized (Fig. 11A). This is quickly followed by the development of two macroscopic fracture zones in the post-peak regions (Fig. 11 B). Finally, the interior macroscopic fracture zone forms and becomes interconnected to form an inverse V-shaped open fracture (Fig. 11 C). Because of the high properties of the loading plates, the cones are not developed at the two ends of the specimen and the specimen ultimately fails into two parts along an approximate 45-degree plane, with a big block on the right expected to break away from the specimen (Fig. 11 D).

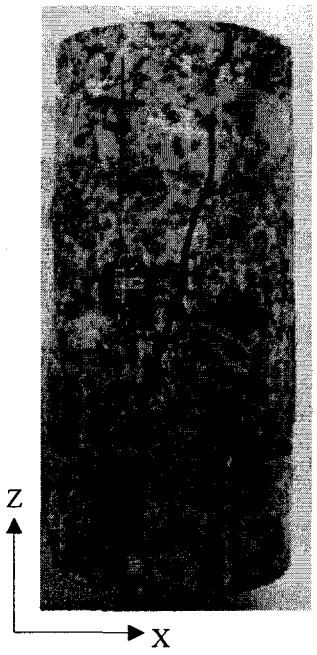

Fig.12 Failed rock specimen

The failed rock specimen is shown in Fig. 12, which shows that the propagation of the crack is similar to the AE source location shown in Fig. 6(b)

5. Conclusion

In this work, the measurements of acoustic emission and the source location were conducted on granite specimens under uniaxial compression. The numerical analysis wasalso conducted using numerical tool RFPA code coupled with a heterogeneous and anistropic material. It was shown that the simulated results using RFPA code were similar tendency to the experimental results and could obtain the crack initiation, propagation, and whole progressive fracture process.

Acknowledgements

The study presented in this paper was partly supported by grants from the Korea-China Young Scientist Exchange Program (2004) of the KOSEF(Korea Science and Engineering Foundation); the NNSF, China

■ References ■

[1] Chang S. -H. and Lee C. -I. Estimation of cracking and damage mechanisms in rock under triaxial compression by moment tensor analysis of acoustic emission, International Journal of Rock Mechanics and Mining Sciences, Volume 41, Issue 7, October 2004, Pages 1069-1086

[2] Eberhardt E. Brittle Rock Fractures and Progressive Damage in Uniaxial compression. Ph.D. thesis, University of Saskatchewan, 1998.

[3] EberhardtE, Stead D, Stimpson B. Quantifying progressive prepeak brittle fracture damage in rock during uniaxial compression. Int J Rock Mech Min Sci 1999;36(3):36180

[4] Falls SD, Young RP. Acoustic Emission and ultrasonic-velocity methods used to characterise the excavation disturbance associated with deep tunnels in hard rock. Tectonophysics, 1998;289(13):115

[5] Lavrov A., Vervoort A., Wevers M. and Napier J. A. L., Experimental and numerical study of the Kaiser effect in cyclic Brazilian tests with disk rotation, International Journal of Rock Mechanics and Mining Sciences, Volume 39, Issue 3, April 2002, Pages 287-302

[6] Alexander Lavrov, Kaiser effect observation in brittle rock cyclically loaded with different loading rates, Mechanics of Materials, Volume 33, Issue 11, November 2001, Pages 669-677

[7] Lavrov A.,The Kaiser effect in rocks: principles and stress estimation techniques, International Journal of Rock Mechanics and Mining Sciences, Volume 40, Issue 2, February 2003, Pages 151-171

[8] Bing Chen and Juanyu Liu, Experimental study on AE characteristics of three -point-bending concrete beams, Cement and Concrete Research, Volume 34, Issue 3, March 2004, Pages 391-397

[9] Liu H. Y., Roquete M., Kou S. Q. and Lindqvist P. -A., Characterization of rock heterogeneity and numerical verification, Engineering Geology, Volume 72, Issues 1-2, March 2004, Pages 89-119

[10] Liu H.Y., Kou S.Q. and Lindqvist P.-A., Numerical studies on the inter-particle breakage of a confined particle assembly in rock crushing, Mechanics of Materials, Volume 37, Issue 9, September 2005, Pages 935-954

[11] Tang C A, Numerical simulation of progressive rock failure and associated seismicity, International Journal of Rock Mechanics and Mining Sciences, Volume 34, Issue 2, February 1997, Pages 249-261

[12] Wang S. H., Liu J. X., Tang C. A., Li L. C. and Zhao X. D. Stability analysis of a large-span and deep tunnel, International Journal of Rock Mechanics and Mining Sciences, Volume 41, Supplement 1, May 2004, Pages 870-875